AIAA JOURNAL
Vol. 33, No. 7, July 1995

Pointwise Energy Release Rate in Delaminated Plates

B. V. Sankar* and V. Sonik†
University of Florida, Gainesville, Florida 32611

A laminated plate theory suitable for analyzing delaminations has been derived. The theory is used to study the interaction between the top and bottom sublaminates in the intact region of a delaminated plate. Expressions are derived for the jump in force and moment resultants that occur across the delamination front. Using Irwin's crack closure integral, a simple expression for pointwise strain energy release rate G along the delamination front has been derived. The expression suggests that the G at any point on the delamination front is the difference between the plate strain energy densities behind and ahead of the delamination front. An estimate of error in computing G using plate theories is obtained by comparing the J integral obtained using exact stress fields and plate stresses. The procedure for computing G is first verified by applying it to double cantilever beam specimens (DCB) and elliptical delaminations in isotropic plates for which solutions are available or can be computed. Then the method is illustrated for a stitched graphite/epoxy DCB specimen and also for elliptical delaminations in 0-deg graphite/epoxy plates. The results demonstrate the usefulness of the present method in analyzing delaminated coupons and structures.

I. Introduction

DELAMINATIONS in composite laminates can occur during fabrication or service, e.g., low-velocity impact. One way of avoiding the deleterious effects of delamination is frequent inspection and repair/replacement, which is very expensive. On the other hand the structures can be designed to be damage tolerant. Since most of the delaminations propagate in the same plane, fracture mechanics principles can be successfully applied to determine the loads at which a delamination will begin to grow. The strain energy release rate G has been widely accepted as the fracture parameter that characterizes delamination propagation. In the case of three-dimensional structures, G has to be computed at every point on the delamination front, i.e., "pointwise G" has to be evaluated. This strictly requires three-dimensional analysis, which can be quite expensive for practical problems. However, in many applications laminated composites are used in the form of plate-like structures, and we can take advantage of the plate theories to compute the strain energy release rate distribution along a delamination front. A similar approach has been used for beams by various authors.[1–6] Recently, Sankar and Rao,[7] Davidson,[8] and Davidson and Krafchak[9] have extended the method to plate problems. In the present paper we derive simple expressions for the strain energy release rate distribution in terms of the strain energy density of the sublaminates computed using plate theories.

The issues involved in computing G from the three-dimensional analysis have been discussed in detail by Atluri and Nishioka[10] and Shih et al.[11] and summarized by Anderson.[12] The G at a point on the delamination front can be computed by evaluating the J integral on a vanishingly small contour that lies on the plane perpendicular to both the plane of delamination and the tangent to the delamination front at the point in consideration.

In plane problems the difficulties in evaluating the aforementioned integral can be avoided by taking advantage of the path-independent nature of the integral.[13] However, this is not possible in three-dimensional problems. Shih et al.[11] suggest a domain integral representation of the aforementioned integral that is much suited to finite element analysis. Banks-Sills[14] has conducted an extensive study of use of three-dimensional finite elements in linear elastic fracture mechanics (LEFM).

In the present study we have focused our attention on issues involved in computing pointwise G using laminated plate theories. The emphasis is on rigorous derivation of jump conditions across the delamination front and also the equivalence of the plate models and three-dimensional analysis. A simple expression for pointwise G in terms of the plate strain energy densities along the delamination front has been derived. The method is verified by solving problems for which solutions are available and then demonstrated for some complex structures, including laminates with through-the-thickness reinforcements.

II. Preliminaries

In this section we derive the constitutive relations and equilibrium equations for a laminated plate. The treatment is slightly different from the traditional approaches in which the middle plane of the plate is used as the reference plane for defining the displacement field. In the present approach the top or bottom plane of the plate is used as the reference x_1x_2 plane. The derivations will mainly refer to a plate situated just above the reference plane, i.e., the plate is bounded by the planes $x_3 = 0$ and h (see Fig. 1).

The case where the plate surfaces are $x_3 = 0$ and $-h$ can be treated in an analogous manner. We will include the transverse shear deformation as well as the thickness stretch mode introduced by Whitney.[15] Both indicial and vector notations are used for stresses, force resultants, etc., in this paper, depending on the convenience of presentation. In the following an underscore denotes a matrix, $\lfloor\cdot\rfloor$ denotes a row matrix, a superscripted T denotes matrix transpose, and a suffix preceded by a comma denotes differentiation. The displacement field in the plate is approximated by

$$u_i(x_1, x_2, x_3) = U_i(x_1, x_2) + x_3\theta_i(x_1, x_2), \qquad (i = 1, 2, 3) \tag{1}$$

The various U_i are displacement of points on the reference plane, θ_1 and θ_2 are the rotations, and θ_3 is the thickness stretch, θ_3 is set to zero, and we recover the standard shear deformation theory. The strain field can be represented as

$$\underline{\epsilon} = \underline{\epsilon}_0 + x_3\underline{\kappa} \tag{2}$$

Received March 7, 1994; presented as Paper 94-1398 at the AIAA/ASME/ASCE/AHS/ASC 35th Structures, Structural Dynamics, and Materials Conference, Hilton Head, SC, April 18–20, 1994; revision received Sept. 20, 1994; accepted for publication Sept. 24, 1994.

*Associate Professor, Department of Aerospace Engineering, Mechanics, and Engineering Sciences, Center for Studies of Advanced Structural Composites. Member AIAA.

†Graduate Student, Department of Aerospace Engineering, Mechanics, and Engineering Sciences, Center for Studies of Advanced Structural Composites. Member AIAA.

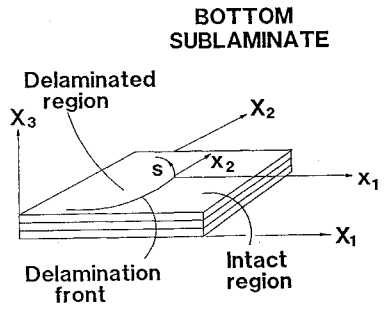

Fig. 1 Crack front in a delaminated plate.

where

$$\underline{\epsilon}^T = \lfloor \epsilon_{11} \quad \epsilon_{22} \quad \epsilon_{33} \quad \gamma_{23} \quad \gamma_{31} \quad \gamma_{12} \rfloor \tag{3}$$

$$\underline{\epsilon}_0^T = \lfloor U_{1,1} \quad U_{2,2} \quad \theta_3 \quad (\theta_2 + U_{3,2}) \quad (\theta_1 + U_{3,1}) \quad (U_{1,2} + U_{2,1}) \rfloor \tag{4}$$

$$\underline{\kappa}^T = \lfloor \theta_{1,1} \quad \theta_{2,2} \quad 0 \quad \theta_{3,2} \quad \theta_{3,1} \quad (\theta_{1,2} + \theta_{2,1}) \rfloor \tag{5}$$

The force and moment resultants are defined as

$$(N_{ij}, M_{ij}) = \int_0^h \sigma_{ij}\,(1, x_3)\,dx_3, \qquad (i, j = 1, 2, 3) \tag{6}$$

It should be mentioned that the limits of integration in Eq. (6) are 0 and h, and hence the moment resultants are about an axis on the reference x_1x_2 plane. It will be sometimes convenient to denote the stresses and the force and moment resultants as pseudovectors σ, $\underline{N}$, and $\underline{M}$ containing elements σ_α, N_α, and M_α, respectively. The relation between the two sets of notations, e.g., N_α and N_{ij}, is given by $\alpha = i$ for $i = j$, and $\alpha = 9\text{-}i\text{-}j$ otherwise. In that case the force and moment resultants are

$$(\underline{N}, \underline{M}) = \int_0^h \underline{\sigma}(1, x_3)\,dx_3 \tag{7}$$

The stress-strain relations are

$$\underline{\sigma} = \underline{c}\,\underline{\epsilon} \tag{8}$$

Using Eqs. (2), (7), and (8), one can derive the laminate constitutive relations as

$$\begin{pmatrix} \underline{N} \\ \underline{M} \end{pmatrix} = \begin{bmatrix} \underline{A} & \underline{B} \\ \underline{B} & \underline{D} \end{bmatrix} \begin{pmatrix} \underline{\epsilon}_0 \\ \underline{\kappa} \end{pmatrix} \tag{9}$$

where the various stiffness matrices of the laminate are given by

$$(\underline{A}, \underline{B}, \underline{D}) = \int_0^h \underline{c}\left(1, x_3, x_3^2\right) dx_3 \tag{10}$$

By denoting the force and moment resultants as $\underline{F}$, the plate deformations as $\underline{E}$, and the laminate stiffness as $\underline{C}$, Eq. (9) can be written in a shorthand notation as $\underline{F} = \underline{C}\,\underline{E}$.

The stress equilibrium equations (neglecting body forces) are

$$\sigma_{ij,j} = 0, \qquad (i, j = 1, 2, 3) \tag{11}$$

Integrating Eq. (11) through the thickness of the plate we obtain

$$N_{i\alpha,\alpha} + t_i = 0, \qquad (i = 1, 2, 3;\ \alpha = 1, 2) \tag{12}$$

where t_i are the sum of surface tractions acting on the top and bottom surfaces of the plate:

$$t_i = \sigma_{3i}(x_1, x_2, h) - \sigma_{3i}(x_1, x_2, 0) \tag{13}$$

By multiplying Eq. (11) by x_3 throughout and integrating through the thickness, we obtain

$$M_{i\alpha,\alpha} + m_i - N_{i\beta} = 0, \qquad (i = 1, 2, 3;\ \alpha = 1, 2) \tag{14}$$

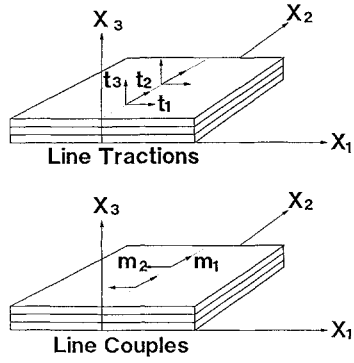

Fig. 2 Line tractions and couples on the bottom sublaminate.

where the various moments m_i are given by

$$m_i = h\sigma_{3i}(x_1, x_2, h) \tag{15}$$

The previous equation derived from the stress equilibrium equations does not account for distributed couples that can be applied onto a plate. In fact, there are two sets of couples that can be applied: $\mu_1(x_1, x_2)$ about the x_1 axis and $\mu_2(x_1, x_2)$ about the x_2 axis. They can be added to the couples m_1 and m_2 in Eq. (14). Because the sign conventions for the various m and μ are different, μ_2 has to be added to m_1 and μ_1 to $-m_2$. A couple about the x_3 axis cannot be applied because we do not have rotation about the x_3 axis as a degree of freedom (drilling DOF) in the present plate theory. The plate strain energy density Φ is defined as the strain energy per unit area of the plate:

$$\Phi = \int_0^h \left(\tfrac{1}{2}\right)\underline{\epsilon}^T \underline{c}\,\underline{\epsilon}\ dx_3 \tag{16}$$

where the integrand is the strain energy density at a point in the plate. By substituting from Eqs. (2) and (10) into Eq. (16), we can derive the following two expressions for Φ:

$$\Phi = \left(\frac{1}{2}\right)\underline{F}^T\underline{E} \tag{17}$$

When concentrated forces and couples act on the plate, they lead to jump in the force and moment resultants. In the following we derive a relationship between forces and couples acting along a line and the jump in force and moment resultants across that line. Consider that a set of line forces and line couples act along the line $x_1 = 0$ as shown in Fig. 2 such that

$$t_i(x_1, x_2) = f_i(x_2)\delta(x_1) \qquad (i = 1, 2, 3) \tag{18}$$

$$m_i(x_1, x_2) = g_i(x_2)\delta(x_1) \qquad (i = 1, 2) \tag{19}$$

where δ is the Dirac delta function.

Substituting for t_i from Eq. (18) into Eq. (12) and integrating from $-\Delta x_1$ to $+\Delta x_1$ we obtain

$$\int_{-\Delta x_1}^{+\Delta x_1} N_{i1,1}\,dx_1 + \int_{-\Delta x_1}^{+\Delta x_1} N_{i2,2}\,dx_1 + f_i \int_{-\Delta x_1}^{+\Delta x_1} \delta(x_1)\,dx_1 = 0, \qquad (i = 1, 2, 3) \tag{20}$$

Taking the limit as $\Delta x_1 \to 0$,

$$\{N_{i1}\} + f_i = 0, \qquad (i = 1, 2, 3) \tag{21}$$

where $\{\cdot\}$ denotes the jump in the function inside the braces across the line $x_1 = 0$. Similarly, using Eqs. (14) and (19), one can show that

$$\{M_{i1}\} + g_i = 0, \qquad (i = 1, 2) \tag{22}$$

The derivations given thus far pertain to a laminate situated just above the reference plane. For a laminate situated just below the reference plane the only change will be in the limits of integration in Eqs. (6), (7), and (10), from $-h$ to 0 instead of 0 to h.

III. Analysis of a Delaminated Plate

We propose to use the plate theory developed herein for the analysis of delaminated plates, in particular to compute the strain energy release rate distribution $G(s)$ along the delamination front. We assume that 1) the delaminated sublaminates and the parent laminate are large enough compared with the plate thickness, 2) the delamination front is a smooth curve without any sharp corners or discontinuities, and 3) the distance between any point of application of external loads and the delamination front is large compared with the plate thickness. If these assumptions are valid, then the displacement of points away from the delamination front computed using the plate theory will be sufficiently accurate and hence the estimate of total strain energy in the entire plate. The delaminated plate can be considered as consisting of two laminates, the top and bottom, separated in the region of delamination, and connected to each other (intact) elsewhere (see Fig. 1). The delamination plane is used as the reference plane (x_1x_2 plane) for deriving the equations of the top and bottom sublaminates and also the intact laminate.

Next we look at the nature of interaction between the top and bottom laminates in the undelaminated (intact) region. Let $\underline{C}^{(t)}$ and $\underline{C}^{(b)}$ be the stiffnesses of the top and bottom sublaminates, respectively. Then it is obvious from the definition of $\underline{C}$ in Eq. (10) that the stiffness of the intact plate $\underline{C} = \underline{C}^{(t)} + \underline{C}^{(b)}$. This is because the limits of integration for the intact plate is from $-h_b$ to $+h_t$, which then represents the sum of integrals for the top and bottom sublaminates. Let $\underline{F}$, $\underline{F}^{(t)}$, and $\underline{F}^{(b)}$ be the force and moment resultants in the intact, top, and bottom laminates respectively. From the definition of force and moment resultants in Eq. (7) it can be seen that $\underline{F} = \underline{F}^{(t)} + \underline{F}^{(b)}$. The deformations in the top and bottom plate are the same and equal to the deformation of the intact plate, i.e., $\underline{E}^{(t)} = \underline{E}^{(b)} = E$. From these the reaction between the force resultants in the top laminate $\underline{F}^{(t)}$ and the total force resultants $\underline{F}$ can be written as

$$\underline{F}^{(t)} = \underline{C}^{(t)}\,\underline{C}^{-1}\,\underline{F} \tag{23}$$

Thus one can see that the force resultants in the top (or bottom) laminate are a linear combination of the force resultants acting on the intact plate. Thus, as long as no singular external tractions or couples act on the plate, the interaction between the top and bottom laminates in the intact region is characterized by smooth and nonsingular tractions and couples.

Next we will consider the situation near the delamination front. For the purpose of convenience we will assume that the delamination front is locally tangential to the x_2 axis as shown in Fig. 1. Because the deformations can be different in the top and bottom sublaminates behind the crack front, there will be discontinuities (jumps) in the forces at the crack front. These jumps can be related to the line forces and couples acting between the two sublaminates at the crack front. Referring to Fig. 3 and Eqs. (21) and (22), the jump in the force resultants can be expressed as

$$f_i = \left[N_{i1}^{(3)} - N_{i1}^{(4)}\right] = \left[N_{i1}^{(1)} - N_{i1}^{(2)}\right], \qquad (i = 1, 2, 3) \tag{24}$$

$$g_i = \left[M_{i1}^{(3)} - M_{i1}^{(4)}\right] = \left[M_{i1}^{(1)} - M_{i1}^{(2)}\right], \qquad (i = 1, 2) \tag{25}$$

In deriving the previous two expressions, we have used the equilibrium relation

$$\underline{F}^{(1)} + \underline{F}^{(4)} = \underline{F}^{(2)} + \underline{F}^{(3)} \tag{26}$$

Next we apply Irwin's crack closure integral[16] to compute the strain energy release rate. We will allow the crack front to grow by an arbitrary distance $\Delta l(s)$ along the crack front. Consider a small portion of the delamination front that is locally tangential to the x_2 axis as shown in Fig. 1. Let its length be Δs. We will compute the work done in closing this small portion of the crack. In applying virtual crack closure principle we consider the tractions acting in between the impending crack surfaces over a small area ahead of the crack and multiply by the relative crack surface opening displacements at corresponding points behind the crack, and take the limit as this area or crack extension tends to zero. In doing so the work due to the distributed tractions and couples will vanish unless they exhibit a singular behavior at the crack tip. We have shown

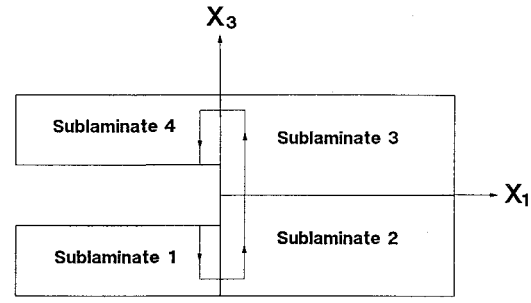

Fig. 3 Zero-area path for computing the J integral.

in the beginning of this section [Eq. (23)] that the tractions and couples acting between the sublaminates in the intact plate have regular behavior. Therefore, they will not contribute to the crack closure virtual work. However, there are line tractions and couples acting along the crack front, and these will contribute to the virtual work term. Thus, the work done is given by

$$\Delta W = \left(\tfrac{1}{2}\right)\Delta s \sum_{i=1}^{3} f_i\left[U_i^{(4)}(-\Delta l, x_2) - U_i^{(1)}(-\Delta l, x_2)\right]$$

$$+\left(\tfrac{1}{2}\right)\Delta s \sum_{i=1}^{2} g_i\left[\theta_i^{(4)}(-\Delta l, x_2) - \theta_i^{(1)}(-\Delta l, x_2)\right] \tag{27}$$

By adding and subtracting $U_i(0, x_2)$ and $\theta_i(0, x_2)$ in Eq. (27), we obtain

$$\Delta W = \left(\tfrac{1}{2}\right)\Delta s \sum_{i=1}^{3} f_i\left[U_i^{(4)}(-\Delta l, x_2)\right.$$

$$\left. - U_i(0, x_2) - U_i^{(1)}(-\Delta l, x_2) + U_i(0, x_2)\right]$$

$$+\left(\tfrac{1}{2}\right)\Delta s \sum_{i=1}^{2} g_i\left[\theta_i^{(4)}(-\Delta l, x_2) - \theta_i(0, x_2)\right.$$

$$\left. - \theta_i^{(1)}(-\Delta l, x_2) + \theta_i(0, x_2)\right] \tag{28}$$

We define the strain energy release rate computed from the plate theory G_p as

$$G_p = \lim_{\substack{\Delta l \to 0 \\ \Delta s \to 0}} \frac{\Delta W}{\Delta l \Delta s} \tag{29}$$

Substituting for ΔW from Eq. (28) into Eq. (29), we obtain

$$G_p = \left(\frac{1}{2}\right)\sum_{i=1}^{3}\left[N_{i1}^{(4)} - N_{i1}^{(3)}\right]\left[U_{i,1}^{(4)} - U_{i,1}^{(1)}\right]$$

$$+\left(\frac{1}{2}\right)\sum_{i=1}^{2}\left[M_{i1}^{(4)} - M_{i1}^{(3)}\right]\left[\theta_{1,1}^{(4)} - \theta_{i,1}^{(1)}\right] \tag{30}$$

In deriving Eq. (30) we have used Eqs. (24) and (25) and also the definition of the derivative of displacements, e.g.,

$$U_{i,1}^{(4)} = \lim_{\Delta l \to 0} \frac{U_i(0, x_2) - U_i^{(4)}(-\Delta l, x_2)}{\Delta l} \tag{31}$$

We will use the force equilibrium Eq. (26) and also the fact that the deformations in sublaminates 2 and 3 are the same, i.e., $\underline{E}^{(2)} = \underline{E}^{(3)}$, to modify Eq. (30) as follows:

$$G_p = \left(\frac{1}{2}\right)\sum_{i=1}^{3}\left[N_{i1}^{(4)} - N_{i1}^{(3)}\right]\left[U_{i,1}^{(4)} - U_{i,1}^{(3)}\right]$$

$$+\left[N_{i1}^{(1)} - N_{i1}^{(2)}\right]\left[U_{i,1}^{(1)} - U_{i,1}^{(2)}\right]$$

$$+\left(\frac{1}{2}\right)\sum_{i=1}^{2}\left[M_{i1}^{(4)} - M_{i1}^{(3)}\right]\left[\theta_{i,1}^{(4)} - \theta_{i,1}^{(3)}\right]$$

$$+\left[M_{i1}^{(1)} - M_{i1}^{(2)}\right]\left[\theta_{i,1}^{(1)} - \theta_{i,1}^{(2)}\right] \tag{32}$$

In Eq. (32) the sum of the first and third terms on the right-hand side can be written as $[\underline{F}^{(4)} - \underline{F}^{(3)}]^T [\underline{E}^{(4)} - \underline{E}^{(3)}]$, and the sum of the second and fourth terms can be written as $[\underline{F}^{(1)} - \underline{F}^{(2)}]^T [\underline{E}^{(1)} - \underline{E}^{(2)}]$. The explanation for this is as follows. We have already established that only N_{i1} and M_{i1} can be discontinuous across the delamination front. Considering the terms in the deformation vector E, we find U_i and θ_i have to be continuous at the delamination front. In the deformation gradients, the derivatives with respect to x_2 (the delamination front is assumed to be tangential to x_2) have to be unique along the x_2 axis and hence continuous across the delamination front. However, the derivatives with respect to the coordinate normal to the delamination front (x_1 in this case) can be discontinuous. Thus $U_{i,1}$ and $\theta_{i,1}$ can be discontinuous. The terms on the right-hand side of Eq. (32) represent the product of jumps in the force resultants and deformations. By adding the jump in the continuous terms (which is equal to zero) both in the force $\underline{F}$ and deformation $\underline{E}$, we can write Eq. (32) as follows:

$$G_p(s) = \left(\tfrac{1}{2}\right)\left[\underline{F}^{(4)} - \underline{F}^{(3)}\right]^T \left[\underline{E}^{(4)} - \underline{E}^{(3)}\right] + \left(\tfrac{1}{2}\right)\left[\underline{F}^{(1)} - \underline{F}^{(2)}\right]^T \left[\underline{E}^{(1)} - \underline{E}^{(2)}\right] \tag{33}$$

The previous expression can be further simplified by using the equilibrium condition $\underline{F}^{(1)} + \underline{F}^{(4)} = \underline{F}^{(2)} + \underline{F}^{(3)}$, the compatibility condition of the intact laminate, $\underline{E}^{(2)} = \underline{E}^{(3)}$, and the two reciprocal relations $\underline{F}^{(1)T}\,\underline{E}^{(2)} = \underline{F}^{(2)T}\,\underline{E}^{(1)}$ and $\underline{F}^{(4)T}\,\underline{E}^{(3)} = \underline{F}^{(3)T}\,\underline{E}^{(4)}$. [The reciprocal relations are the direct consequence of symmetry of the laminate stiffness matrix $\underline{C}$ and also the fact that $\underline{C}^{(1)} = \underline{C}^{(2)}$ and $\underline{C}^{(3)} = \underline{C}^{(4)}$]. The simplified version of Eq. (33) is

$$G_p(s) = \Phi^{(1)} + \Phi^{(4)} - \Phi^{(2)} - \Phi^{(3)} \tag{34}$$

In arriving at Eq. (34) we have used Eq. (17) for the laminate strain energy density. Stated in words, the strain energy release rate at a point on the delamination front is equal to the difference in the strain energy densities behind and ahead of the front at that point.

Equation (34) represents the pointwise strain energy release rate in the context of the plate theory. We still have to show under what conditions it is equal to the result obtained via three-dimensional analysis. Let the actual strain energy release rate distribution obtained using a three-dimensional analysis be given by $G(s)$. For an arbitrary infinitesimally small delamination growth given by $\Delta l(s)$ the change in strain energy of the entire plate Φ_p is given by

$$\Delta\Phi_p = \oint_s G(s)\Delta l(s)\,\mathrm{d}s \tag{35}$$

where the contour integral is taken around the delamination front. Equation (35) is applicable only for the case where the loads remain constant during the delamination growth. In the context of plate theory we can write a similar expression for change in the plate strain energy as

$$(\Delta\Phi_p)_{PT} = \oint_s \Delta W \tag{36}$$

where ΔW is the crack closure work given by Eq. (27). By multiplying and dividing by $\Delta l(s)\Delta s$ in Eq. (36), taking the limit as $\Delta l(s) \to 0$, and following the procedures used to derive Eqs. (27–34), we obtain

$$(\Delta\Phi_p)_{PT} = \oint_s G_p(s)\Delta l(s)\,\mathrm{d}s \tag{37}$$

According to the assumptions we have made in the previous section regarding the applicability of plate theories for the present problem, the change in strain energy $\Delta\Phi_p$ computed by Eqs. (35) and (37) should be equal for any arbitrary $\Delta l(s)$. This can be true only if $G_p(s)$ is equal to $G(s)$ all along the delamination front.

IV. *J* Integral for Plate Models

In three-dimensional crack problems the J integral is evaluated around a contour Γ that surrounds the crack tip and is vanishingly small:

$$J = \lim_{\Gamma\to 0} \int_\Gamma \left(w\delta_{1j} - \sigma_{ij}u_{i,1}\right)n_j\,\mathrm{d}\Gamma \tag{38}$$

Let the value of the J integral evaluated around an arbitrary path be denoted by J_a. Then J_a does not represent the strain energy release rate. The difference between J_a and J can be derived as (see Appendix)

$$J - J_a = \int_A \frac{\partial(\sigma_{i2}u_{i,1})}{\partial x_2}\,\mathrm{d}A \tag{39}$$

where the previous integral is evaluated over the area enclosed by the path on the x_1x_3 plane (Fig. 1). For plane problems the stresses and strains do not vary along the x_2-axis, and the right-hand side of Eq. (39) will be zero, thus making J_a equal to J for all paths of integration.

It is interesting to note that Sankar and Rao[7] evaluated the J integral around a zero-area path surrounding the crack tip using the stresses and displacements derived using the plate models and obtained an expression for J that was identical to that given by Eq. (34). Let us denote this by J_p to distinguish from the actual J. Now we can derive the error involved in using plate models for computing J (or G). Let us denote the error by J_e:

$$J_e = J_p - J \tag{40}$$

Let us assume that there is a path that is away from the crack tip such that along this path the value of J_{pa} evaluated using plate theories is the same as the actual J_a. Then we can add and subtract this term in Eq. (40) to obtain

$$J_e = (J_p - J_{pa}) - (J - J_a) \tag{41}$$

The terms in parentheses are actually the area integral defined in Eq. (40). Substituting from Eq. (39) into Eq. (41), we obtain

$$J_e = \left[\int_A \frac{\partial(\sigma_{i2}u_{i,1})}{\partial x_2}\,\mathrm{d}A\right]_{\text{plate}} - \left[\int_A \frac{\partial(\sigma_{i2}u_{i,1})}{\partial x_2}\,\mathrm{d}A\right]_{\text{actual}} \tag{42}$$

Equation (42) provides a measure of error in the J or G computed using plate theories [Eq. (34)].

Again in the case of plane problems the area integrals in Eq. (42) vanish and hence the error J_e. Thus we are able to obtain the exact G from beam or one-dimensional plate equations. Thus the only condition that we need to satisfy while using beam models is that there should be at least one cross section in each sublaminate behind and ahead of the crack tip where the stresses match the exact solution. Beam models have been used for computing G in plane structures by several authors.[2,3,5,17]

V. Results and Discussion

Two sets of numerical examples were performed to demonstrate the efficacy of the present method. The first set consisted of examples for which solutions are available or can be computed by other methods, so that the present method of computing G distribution can be verified. The second set of examples illustrates the usefulness of the method in solving some practical delamination problems. All examples were carried out using nine-noded isoparametric plate elements. Each node had 5 DOF, viz., three displacements in the coordinate directions and two rotations derived using the shear deformable laminated plate theory. The thickness stretching term was not included in the examples so as to compare with available results. If the delaminated plate is modeled by more than two sublaminates, then there will be multiple sublaminates above or below the delamination plane. In that case the θ_3 term must be included in the formulation.

The strain energy release rate distribution along the crack front in a 0-deg graphite/epoxy double cantilever beam (DCB) is shown in Figs. 4 and 5. The dimensions and material properties are shown

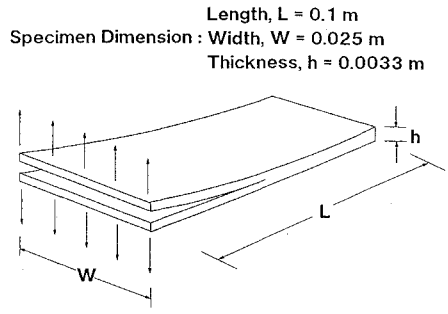

Fig. 4 Double cantilever beam subjected to end loads.

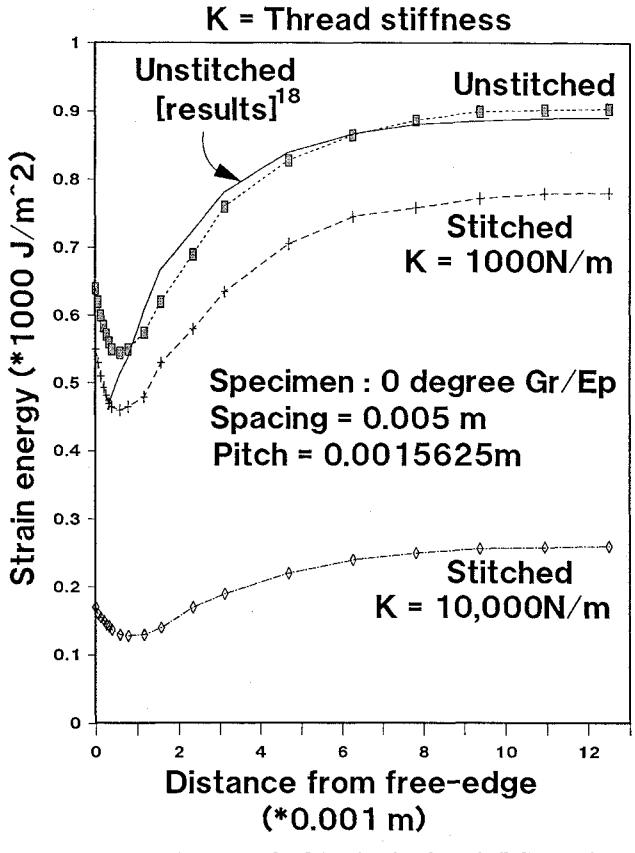

Fig. 5 *G* distribution along the delamination front in DCB specimen.

in the figures. Figure 5 also includes the results for laminates with through-the-thickness stitching, which will be discussed later. From the results for the unstitched laminate one can note that the G is higher at the center of the laminate and drops to a lower value toward the edge. This is similar to the behavior observed by Raju et al.[18] using a three- dimensional finite element analysis. This also explains the thumbnail shape that a straight delamination acquires in DCB specimens. It should be mentioned that we have used contact elements in the vicinity of the specimen edge to avoid interpenetration of the nodes of top and bottom sublaminates of the DCB, and this has resulted in a smooth variation of G unlike that in Ref. 7.

The second example is an isotropic square plate containing an elliptical delamination subjected to a pair of point forces normal to the plate at the center of the ellipse. The plate size is 75 × 75 × 3.3 mm. The delamination is assumed to be in the midplane of the plate. The minor axis of the delamination is kept constant at 15 mm, and the ratio of the major to minor axis varies from 1 to 3. The G distributions in the first quadrant of the delamination are shown in Fig. 6 for various aspect ratios. Since no closed-form results for G are available except for the circular delamination, we used an indirect method to verify the results. The strain energy in a clamped elliptical plate subjected to a central point force can be derived as

$$\Phi_p = \left(\tfrac{1}{2}\right) P w_0 \tag{43}$$

Table 1 Comparison of results for elliptical delaminations

	Aspect ratio, $AR = a/b$		
	1	2	3
$W_{0(\mathrm{FEM})}$, $*10^{-5}$ m	5.75	7.62	7.82
$W_{0(\mathrm{exact})}$, $*10^{-5}$ m	6.08	7.51	7.98
$\Delta\Phi_{(\mathrm{FEM})}$, N-m	2.71	3.62	3.81
$\Delta\Phi_{(\mathrm{exact})}$, N-m	3.34	3.93	4.21

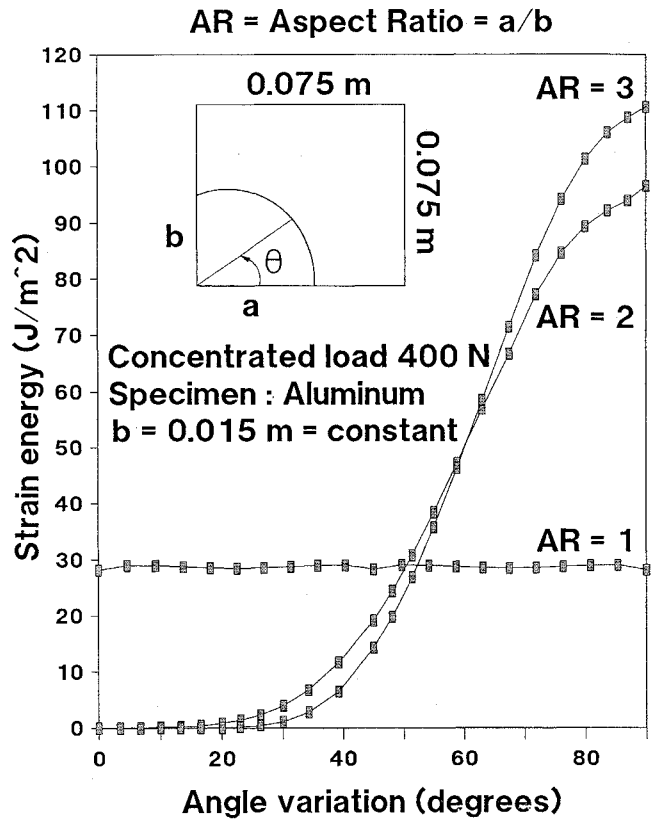

Fig. 6 *G* distribution along elliptical delaminations in isotropic plates.

where P is the load and w_0 is the central deflection given by Young[19]:

$$w_0 = \frac{Pb^2(1-\nu^2)}{Eh^3}(0.34773 - 0.110933\alpha) \tag{44}$$

In the previous equation b is the minor axis, a is the major axis, $\alpha = b/a$, h is the plate thickness, and E and ν are Young's modulus and Poisson's ratio. Let us assume that the delamination grows by an arbitrary small distance Δl as the load P remains constant. (Δl is assumed to be constant along the delamination front). The change in strain energy of the plate can be computed by two different methods. The simpler method involves differentiation of the expression for the strain energy. Thus

$$\Delta\Phi_p = 2\left(\tfrac{1}{2}\right) P\left(\frac{\partial w_0}{\partial a}\Delta l + \frac{\partial w_0}{\partial b}\Delta l\right) \tag{45}$$

The factor 2 in the previous equation is to account for the two sublaminates of the plate. This method can be considered as an exact one to compute the change in strain energy. The second method of computing the change in strain energy due to delamination growth is via fracture mechanics using Eq. (35). Since $\Delta l(s)$ is constant along the delamination front, it can be taken out of the integral sign in Eq. (35). By comparing this expression with Eq. (45), we obtain

$$\oint_s G(s)\,\mathrm{d}s = P\left(\frac{\partial w_0}{\partial a} + \frac{\partial w_0}{\partial b}\right) \tag{46}$$

Thus the comparison of the two terms in the previous equation is a measure of accuracy of the present method for computing $G(s)$. The results are given for various aspect ratios of the ellipse in Table 1.

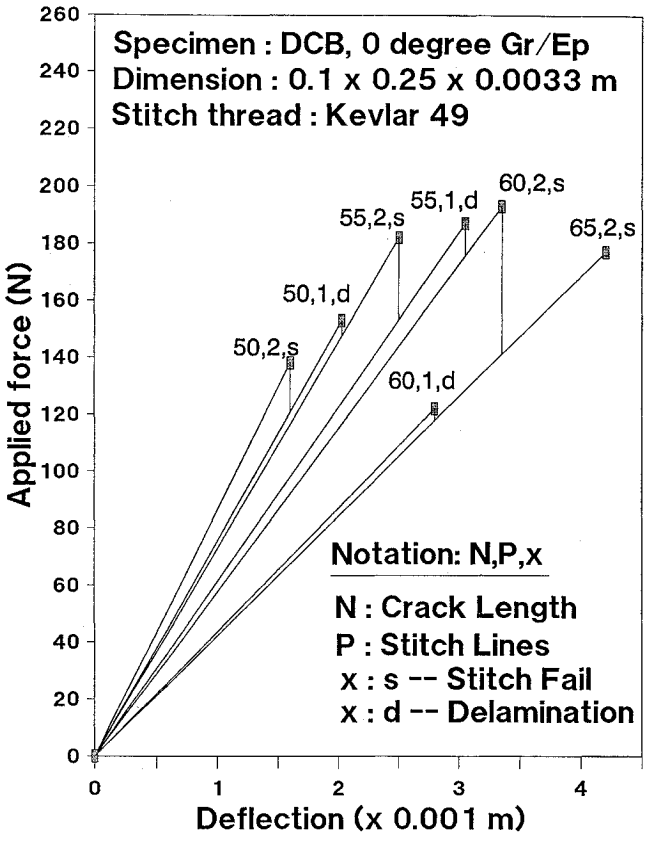

Fig. 7 Progressive damage in stitched DCB specimens.

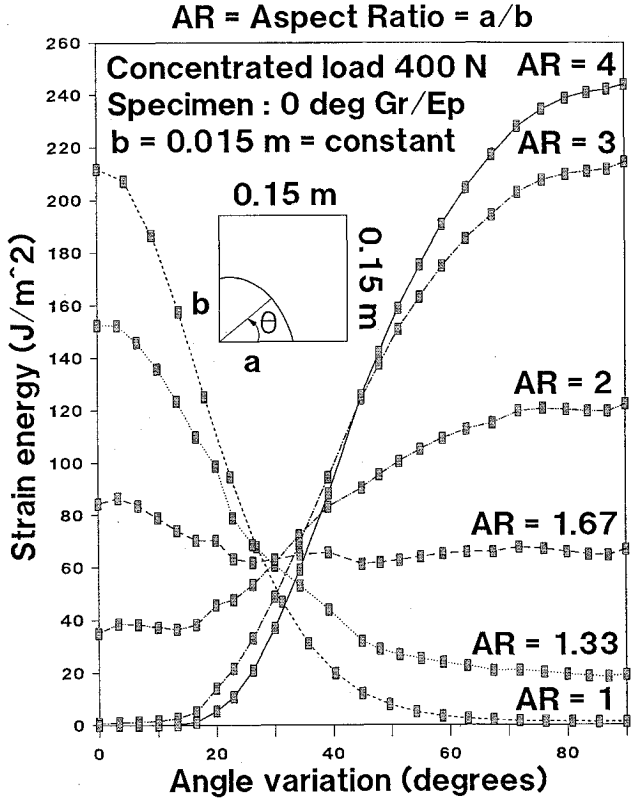

Fig. 8 G distribution along delaminations with different aspect ratios in unidirectional graphite/epoxy plates.

From the results it may be seen that the central deflections from the FEM compare very well with exact solutions, and the comparison for $\Delta\Phi_p$ is reasonable.

Having verified that the plate models work well for delaminated plates, we applied the present method of computing $G(s)$ to two problems: 1) effects of stitches in reducing the strain energy release rate, and 2) strain energy release rate in orthotropic plates due to elliptical delaminations. The DCB specimen shown in Fig. 4 was assumed to have through-the-thickness stitches. The stitches in the delaminated region were modeled using uniaxial bar elements with stiffnesses 1000 and 10,000 N/m. The stitch spacing and pitch are given in Fig. 5. The $G(s)$ was computed using Eq. (34). It may be seen from Fig. 5 that the stitching has a profound effect on reducing the strain energy release rate in delaminated specimens. Figure 7 depicts the load-deflection curve of a DCB specimen during progressive failure of stitches and delamination propagation.

Figure 8 depicts the variation of G in a 0-deg graphite/epoxy laminate due to elliptical delaminations. The delamination is subjected to a pair of opening forces at the center. The results are shown only for the first quadrant of the ellipse. It may be noted that for a circular delamination (aspect ratio $AR = 1$) the G is much higher at $\theta = 0$, and hence there will be a propensity for the crack to propagate along the 0-deg direction and become an elliptical delamination. When the aspect ratio a/b is approximately 1.67, the $G(s)$ is almost constant along the delamination front, and the crack may grow in a self-similar manner thereafter. In fact, elliptical delamination of any arbitrary aspect ratio will eventually change shape to attain this particular aspect ratio.

VI. Conclusions

A simple expression for the pointwise strain energy release rate G along the delamination front has been derived using Irwin's crack closure technique. The expression suggests that the G at any point on the delamination front is the difference between the plate strain energy densities behind and ahead of the crack front. The present procedure for computing G is first verified by applying to problems for which solutions are known. The efficiency of the method is illustrated for stitched double cantilever beam (DCB) specimens and also for elliptical delaminations in composite plates. The results demonstrate the validity of the present technique in analyzing delaminated coupons and structures.

Appendix

In plane solids where the stresses and strains do not vary along the x_2 axis, the following integral is equal to zero for any closed contour on the x_1x_3 plane:

$$\oint (Wn_1 - T_i u_{i,1})\, dS = 0 \tag{A1}$$

where W is the strain energy density and T_i are the tractions. However, the same is not true for three-dimensional states of stress. For three-dimensional cases we have[20]

$$\frac{\partial W}{\partial x_1} = \frac{\partial W}{\partial \epsilon_{ij}} \frac{\partial \epsilon_{ij}}{\partial x_1} = \sigma_{ij}\epsilon_{ij,1} \tag{A2}$$

Applying divergence theorem to the previous equation, we can show that on any closed surface

$$\int_s (Wn_1 - T_i u_{i,1})\, dS = 0 \tag{A3}$$

Consider a prismatic body enclosed by two identical areas on the x_1x_3 plane separated by a small distance Δx_2. Applying the surface integral in Eq. (49) to this prismatic body, we obtain

$$\Delta x_2 \oint_s (Wn_1 - T_i u_{i,1})\, ds - \Delta x_2 \int_A \frac{\partial(\sigma_{i2}u_{i,1})}{\partial x_2}\, dA = 0 \tag{A4}$$

The first term on the left-hand side of the previous equation is the contribution from the lateral surface given by $n_2 = 0$. The second term is from the bases of the prism given by $n_2 = \pm 1$. Canceling Δx_2 throughout, we obtain

$$\oint_s (Wn_1 - T_i u_{i,1})\, ds = \int_A \frac{\partial(\sigma_{i2}u_{i,1})}{\partial x_2}\, dA \tag{A5}$$

Now consider the closed contour ABCD shown in Fig. A1. This closed contour does not include the crack tip, and hence Eq. (A5)

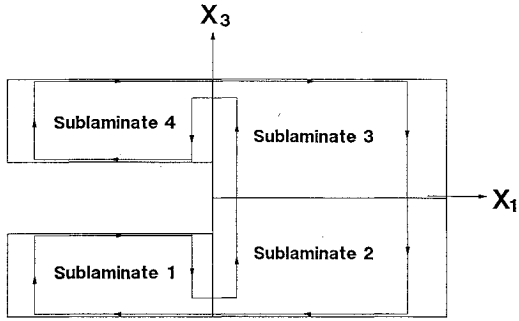

Fig. A1 The zero-area path and an arbitrary path for computing the *J*-integral.

holds good for this contour. The integral on the left-hand side of Eq. (A5) vanishes along the crack surfaces BC and DA. The integral along CD can be written as negative of that along DC. We can recognize the integral along AB as J and that along DC as J_a. Hence Eq. (A5) becomes

$$J - J_a = \int_A \frac{\partial(\sigma_{i2}u_{i,1})}{\partial x_2}\,dA \qquad \text{(A6)}$$

Equation (A6) represents a measure of difference between the zero-area J integral and that evaluated around an arbitrary path surrounding the crack tip. It should be noted that the area integral in Eq. (A6) does not include the crack tip.

Acknowledgments

This research was supported by the NASA Langley Research Center under Grant NAG-1-1226 to the University of Florida. The grant monitor is Wade Jackson. This support is gratefully acknowledged.

References

[1]Schapery, R. A., and Davidson, B. D., "Prediction of Energy Release Rate for Mixed-Mode Delamination Using Classical Plate Theory," *Applied Mechanics Review*, Vol. 43, 1990, pp. S281–S287.

[2]Sankar, B. V., and Hu, S., "Dynamic Delamination Propagation in Composite Beams," *Journal of Composite Materials*, Vol. 25, Nov. 1991, pp. 1414–1426.

[3]Sankar, B. V., "A Finite Element for Modeling Delaminations in Composite Beams," *Computers and Structures*, Vol. 38, No. 2, 1991, pp. 239–246.

[4]Davidson, B. D., and Krafchak, T., "Mixed Mode Energy Release Rate Determination for Delamination Buckling Using Crack-Tip Element," *Proceedings of the AIAA 34th Structures, Structural Dynamics, and Materials Conference*, Pt. 3, AIAA, Washington, DC, 1993, pp. 1302–1309 (AIAA Paper 93-1453).

[5]Sankar, B. V., and Pinheiro, M. A., "An Offset Beam Finite Element for Fracture Analysis of Delaminations," *Proceedings of the AIAA 31st Structures, Structural Dynamics, and Materials Conference*, Pt. 2, AIAA, Washington, DC, 1990, pp. 1227–1233 (AIAA Paper 90-1024).

[6]Sun, C. T., and Pandey, R. K., "A Method for Calculating Strain Energy Release Rate Based on Beam Theory," *Proceedings of the AIAA 34th Structures, Structural Dynamics, and Materials Conference*, Pt. 3, AIAA, Washington, DC, 1993, pp. 1310–1318 (AIAA Paper 93-1454).

[7]Sankar, B. V., and Rao, V. S., "A Plate Finite Element for Modeling Delaminations," *Journal of Reinforced Plastics & Composites*, Vol. 12, Feb. 1993, pp. 227–236.

[8]Davidson, B. D., "Prediction of Delamination Growth in Laminated Structures," *Failure Mechanics in Advanced Polymer Composites*, edited by G. A. Kardomateas and Y. D. S. Rajapakse, AMD-Vol. 196, American Society of Mechanical Engineers, New York, 1994, pp. 43–65.

[9]Davidson, B. D., and Krafchak, T. M., "Analysis of Instability-Related Delamination Growth Using a Crack Tip Element," *AIAA Journal*, Vol. 31, No. 11, 1993, pp. 2130–2136.

[10]Atluri, S. N., and Nishioka, T., "Computational Methods for Three-Dimensional Problems of Fracture," *Computational Methods in the Mechanics of Fracture*, edited by S. N. Atluri, Vol. 2, North-Holland, Amsterdam, 1986, pp. 229–287.

[11]Shih, C. F., Moran, B., and Nakamura, T., "Crack Tip Integrals and Domain Integral Representations for Three-Dimensional Crack Problems," *Analytical, Numerical and Experimental Aspects of Three-Dimensional Fracture Processes*, edited by A. J. Rosakis, K. Ravi-Chandar, and Y. Rajapakse, AMD-Vol. 91, American Society of Mechanical Engineering, New York, 1988, pp. 113–124.

[12]Anderson, T. L., *Fracture Mechanics—Fundamentals and Applications*, CRC Press, Boca Raton, FL, 1991, pp. 659–700.

[13]Rice, J. R., "A Path Independent Integral and the Approximate Analysis of Strain Concentration by Notches and Cracks," *Journal of Applied Mechanics*, Vol. 35, March 1968, pp. 379–386.

[14]Banks-Sills, L., "Use of Three Dimensional Finite Elements in Linear Elastic Fracture Mechanics," edited by A. J. Rosakis, K. Ravi-Chandar, and Y. Rajapakse, AMD-Vol. 91, American Society of Mechanical Engineering, New York, 1988, pp. 89–97.

[15]Whitney, J. M., *Structural Analysis of Laminated Anisotropic Plates*, Technomic Publishing, Lancaster, PA, 1987, pp. 315–319.

[16]Irwin, G. R., "Analysis of Stresses and Strains near the End of a Crack Traversing a Plate," *Journal of Applied Mechanics*, Vol. 24, Sept. 1957, pp. 361–364.

[17]Farris, T. N., and Doyle, J. F., "A Global/Local Approach to Lengthwise Cracked Beams: Static Analysis," *International Journal of Fracture*, Vol. 50, No. 2, 1991, pp. 131–141.

[18]Raju, I. S, Shivakumar, K. N., and Crews, J. H., *AIAA Journal*, Vol. 26, No. 12, 1988, pp. 1493–1498.

[19]Young, W. C., *Roark's Formulas for Stress and Strains*, McGraw-Hill, New York, 1989, p. 440.

[20]Rice, J. R., "Mathematical Analysis in the Mechanics of Fracture," *Fracture*, Vol. II, edited by H. Liebowitz, Academic, New York, 1968, pp. 192–311.